# An evaluation of the stereoscopic capabilities of CORONA declassified spy satellite image data

Nikolaos Galiatsatos, Daniel N. M. Donoghue[1], and Graham Philip[2]

[1]*University of Durham, Department of Geography, South Road, Durham DH1 3LE, UK*
*E-mail:* nikolaos.galiatsatos@durham.ac.uk *and* danny.donoghue@durham.ac.uk
[2]*University of Durham, Department of Archaeology, South Road, Durham, DH1 3LE, UK*
*E-mail:* graham.philip@durham.ac.uk

ABSTRACT: In 1995, a large database of American satellite imagery with worldwide coverage acquired between 1960 and 1972 was declassified. This was the CORONA program imagery and it has proved useful for many applications where image data is difficult to obtain or where historic data is needed. CORONA was the first satellite mission to provide stereoscopic coverage from space and it has already been demonstrated that it is possible to generate digital elevation models (DEMs) from it. The purpose of this paper is to show examples of the quality of elevation data that can be obtained from CORONA stereopairs and to consider the importance of image characteristics (optics, films and filters) which changed with almost every mission and are not widely discussed in the literature. The panoramic geometry of the CORONA cameras is not easily processed by most photogrammetric software packages. The translation of the film data to digital format is also a possible source of error. This research explores the issues surrounding image pre-processing and DEM extraction, and it compares and contrasts the results with other sources of elevation information. The paper also describes problems that are very typical when working in developing countries and it provides a methodology for producing acceptable topographic results.

## 1 INTRODUCTION

The first space satellite to provide stereoscopic coverage was CORONA mission 9031 from 27th of February 1962. The KH-4 design provided along-track stereopairs with a ground resolution of 8 m. The CORONA program continued to provide along-track stereoscopic coverage until 1972, with the designs KH-4A and KH-4B.
This paper discusses the derivation of elevation data from CORONA KH-4B satellite imagery, and assesses the accuracy and resolution of the derived DEM. Erdas OrthoBASE Pro software was used for the triangulation and DEM extraction.
The same software was used by Altmaier & Kany (2002) but in a mountainous landscape in southern Morocco, with DGPS-measured GCPs (Ground Control Points). This contrasts with the relatively flat area of the Homs area in Syria discussed in this paper, where DGPS (Differential Global Positioning System) measurements of "hard points" (simultaneously considered as "sensitive points" by security) could not be applied because of security restrictions. Schmidt *et al.* (2001a) created a DEM from CORONA imagery with the use of VirtuoZo software, again in the same South Morocco area. The accuracy was close to that reported by Altmaier & Kany (2002). Since they cooperated in other papers [Goossens *et al.* (2001), Schmidt *et al.* (2001b)], it can be assumed that the GCPs were derived from the same DGPS measurements (Goossens 2004). None of the above published papers discussed the digitising process in any depth.

## 2 DATA

Although several books about CORONA have been published, e.g. Ruffner (1995), Peebles (1997), McDonald (1997), Day *et al.* (1998), and Madden (1996), all of them focus on the history of CORONA project, and give very little information on photogrammetry problems.
Galiatsatos (2004) demonstrated that no mission was precisely the same as another, and no camera was the same as another. The experiments with cameras, films, filters, slits, lenses and other parts of the satellite systems were continuous. Information taken from declassified CORONA documents such as NRO (1970a) and NRO (1970b) allowed acquisition of the specific satellite system design for the imagery used in this paper (Table 1). There are still some unanswered details, such as whether the alternate or the prime filter was used for the particular frames, or whether the

film is the main one or was spliced-in for the particular frames. Such details may be included in the mission reports in NRO library, but are probably not of vital importance for most applications.

**Table 1 – The particular design of the satellite system for the imagery of the project.**

| Mission | Cameras | Frame No. | Date | Petzval | Film | Filters[$] |
|---------|---------|-----------|------|---------|------|-----------|
| 1108 | Aft | 42,43,44,45 | 17/12/1969 | Type III | 3404 | 25/25 |
| 1110 | Fwd | 07,08,09 | 28/05/1970 | Type II | 3404/14[*] | 21/23A |
| 1110 | Aft | 13,14,15 | 28/05/1970 | Type III | 3404/14[*] | 23A/25 |
| 1111 | Aft | 01,02 | 31/07/1970 | Type III | 3414 | 25/25[¥] |

[$]Prime/Alternate. The most likely filter for the images in the project is the prime. There is uncertainty.
[*]3414 film was spliced-in. There is uncertainty if the film of the project was 3404 or 3414. Most probably it was 3404.
[¥]The alternate filter was glass filter 0.007 inch for increase of 0.001 inch in focus.

From Table 1, it is apparent that the two cameras of mission 1110 have a different generation lens, the forward camera has a second generation and the aft camera a third generation petzval lens. This has an impact on the film resolution. According to NRO (1970a), the performance nadir prediction of the second generation lens is 130 lp/mm and the third generation lens is 155 lp/mm (for a 2.44 msec exposure time, 3404 film type, 2:1 contrast, field angle 0°, and 152 km altitude).

For mission 1110, the overall image quality is less than that provided by previous KH-4B missions (Peebles, 1997). Leachtenauer *et al.* (1997) describe an experiment that tested a sample of CORONA data with both commercial and prototype scanners. They found that the images could be digitised with no loss of information content, but to do so required using a very small digitising spot, which took substantial time and produced large digital files.

Thom (2002) shows that the smaller the step of scan, the better will be the precision and the spatial resolution, but there may also be loss of radiometric precision. In practical applications, the impact of radiometric quality on the geometric precision is not easy to evaluate. Generally, weakly contrasted details can be separated when attention has been given to the radiometric quality. Figure 1 shows the implications of this issue for a scene of high contrast. Furthermore, it demonstrates that when the images are scanned with insufficient care for the radiometric resolution this may result in a loss of detail for applications where contrast is important.
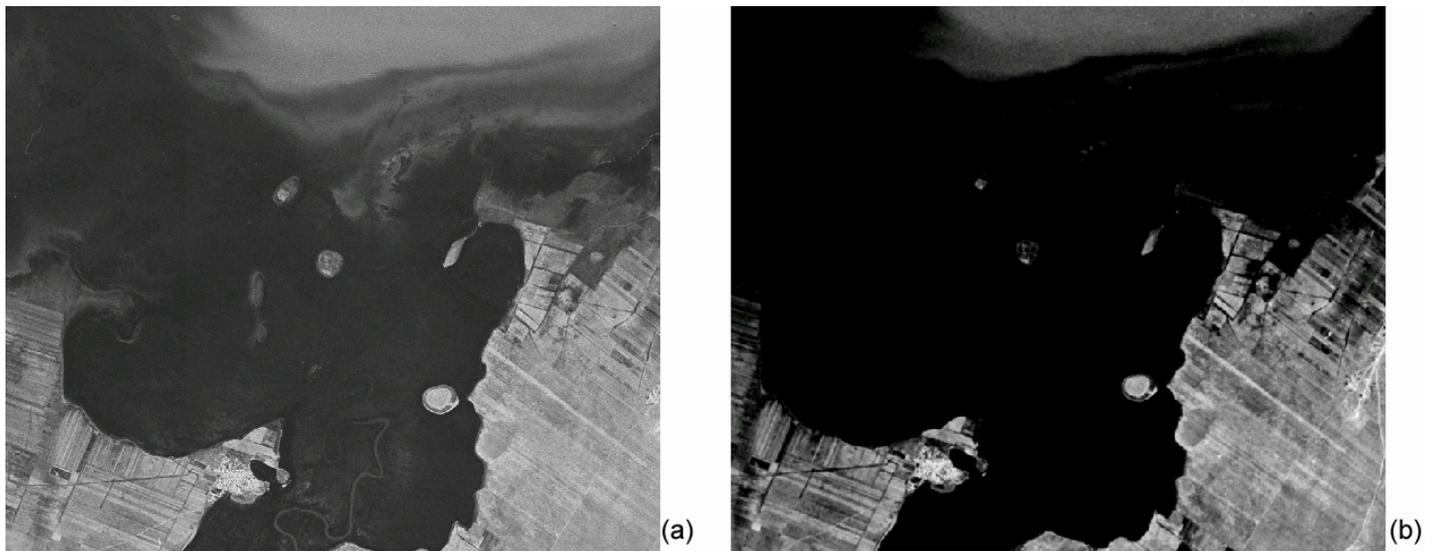


**Figure 1 - Difference in scanning between attention in radiometry detail (a) and attention to geometric precision with high contrast (b).**

This research project used the photogrammetric scanner Vexcel VX4000, and all images were scanned at the optimal 7.5 μm (about 3400 dpi) optical resolution, with attention to radiometric detail.

Tappan *et al.* (2000) preferred to photointerpret CORONA straight from the film without any digitizing. This is a rigorous approach but it inhibits the GIS potential of data integration. Bindschadler & Vornberger (1998) scanned the film to a satisfactory scale for their application, while Palmer (2002) preferred to create prints of larger scale and then scan the prints on a flatbed scanner. Palmer's approach is simple but effective and demonstrates that for certain applications complex data pre-processing may not be necessary.
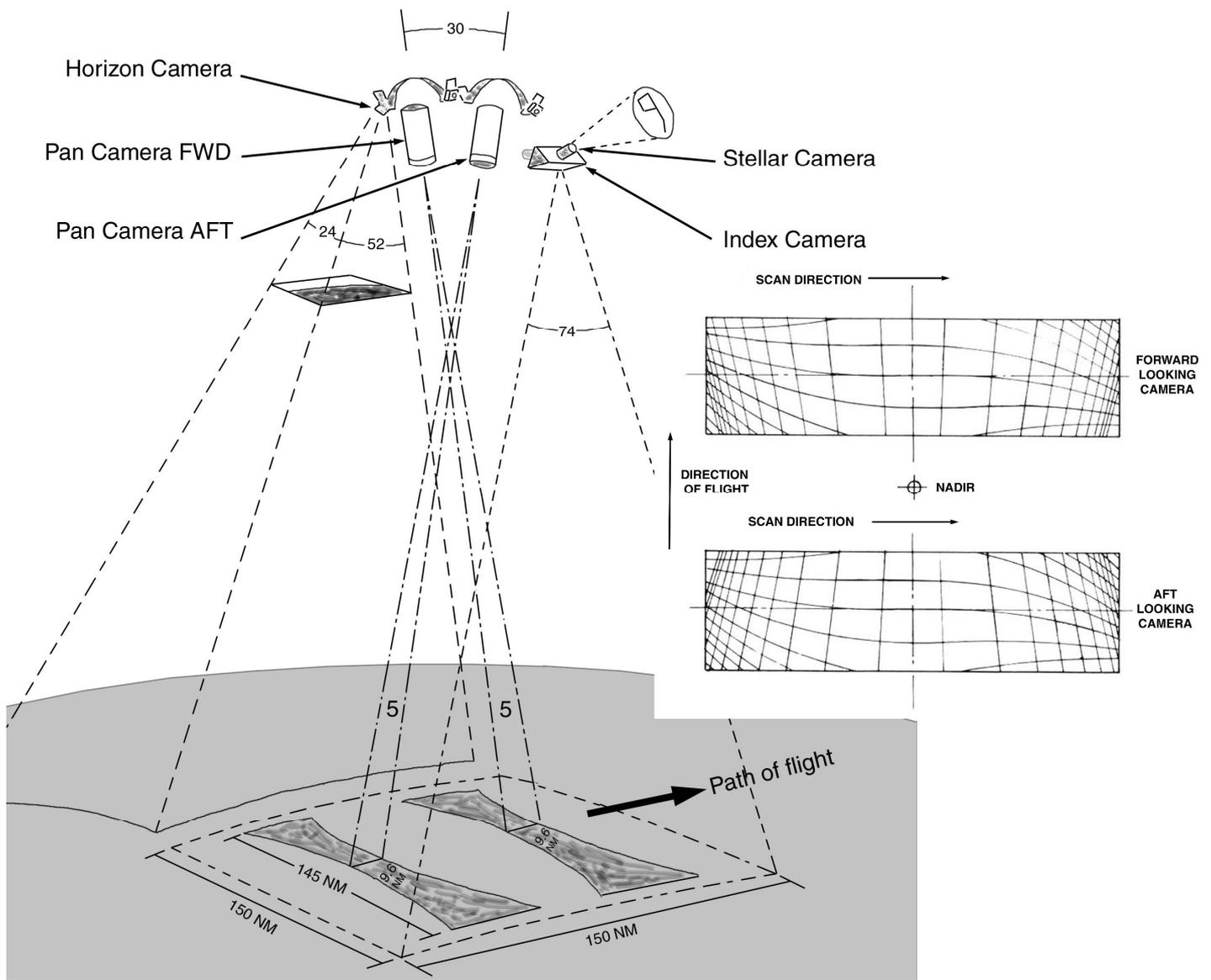
**Figure 2 - CORONA cameras and coverage along with images of a unit grid on the ground obtained with a pair of convergent panoramic cameras in flight (from Slama *et al.*, 1980).**

There are several approaches for the correction of the CORONA data distortions (figure 2). Sohn *et al.* (2004), Schenk *et al.* (2003), and Shin (2003) identify rigorous and other approaches for processing CORONA photography. Panoramic photography was an innovative and fashionable method developed for aerial survey in the 1950s-70s, but it is little used today. The best source of information about these cameras is from publications such as Slama *et al.* (1980) which describe the concepts and the correction of the image data. Note that some of the authors in Slama *et al.* (1980) were involved in the CORONA program. Other important publications are Case (1967) and Devereaux (1973). From the above publications, the most important point is that if there is sufficient ground control then the ephemeris data are not required (Ondrejka, 2000; Slama *et al.*, 1980).

## 3    STUDY AREA

A study area located in the Orontes valley between the cities of Homs and Hama is chosen to illustrate the potential of the CORONA imagery. It extends south of Homs covering a total area of approximately 700 km$^2$; the area is relatively flat, without intense relief; and has an altitudinal range of approximately 400-600 m. The land use is primarily agricultural with small settlements and a lake. This area was chosen for several reasons. First, it is an area with great potential for identifying archaeological sites because it has not been fully explored. In western Syria there has been little acknowledgement of the complexity and sheer diversity of ancient Syrian landscapes, within which the archaeological sites are simply one element. Height data can

greatly assist the process of interpreting potential sites from imagery either directly as in the case of tells[1] or indirectly by providing landscape context. This research was part of a Syrian-British co-operative project organized by the University of Durham and the Directorate General of Antiquities and Museums (DGAM) to study the *Settlement and Landscape Development in the Homs Region* (Philip *et al.*, 2002). One of the aims of the project is to explore the capability of CORONA imagery in comparison to existing topographic mapping (which is 1:25,000 scale) because the application requires the detection of subtle features such as tells, walls, and river terraces. The study also provides a test of a methodology that could be developed and applied through many parts of the world where archaeological resource is currently very poorly documented.

## 4    METHODS

The cameras used on CORONA missions produced panoramic satellite stereo images that were intended to assist manual photo interpretation. Unlike modern satellite stereo image data, it is difficult to obtain the parameters needed to perform a rigorous analysis of digital data to extract height information. It is ironic that the areas of the world where CORONA data is most useful are also the places where it is difficult to obtain accurate ground control points (GCPs) and up to date topographic maps or aerial photos. In areas like the Middle East it is either forbidden or difficult to take measurements to create GCPs and military survey organisations will not provide coordinates, or accurate and comprehensive maps to use as a basemap. For these reasons the following approach was followed.
IKONOS is a satellite sensor with an imaging system free of significant non-linearities (Fraser *et al.*, 2002a). Table 2 shows the geometric properties of IKONOS Panchromatic (1 m spatial resolution) Geo product images acquired over the study area in March 2002. By registering CORONA to the IKONOS Geo product imagery, the CORONA geometry distortions are significantly reduced. Beck *et al.* (in press) show a methodology to improve the accuracy of CORONA geo-location at a local scale. There is also a need to generate height information for GCPs, something that is not included in the IKONOS Panchromatic 1 m resolution imagery. For this, the 1:25,000 Russian military maps were registered to IKONOS, and after registration the heights were sampled from the contour lines. This assumes that the contour lines were produced accurately.

**Table 2 – Directions and angles of CORONA and IKONOS imagery of the project**

| IKONOS | Scan azimuth | Scan direction | Collection azimuth | Collection elevation |
|---|---|---|---|---|
| 756 | 179.97° | Reverse | 38.3713° | 67.22347° |
| 757 | 359.96° | Forward | 67.8092° | 76.36649° |
| | | | | |
| CORONA | Camera looking | Scan direction[*] | Orbit inclination | Sensor elevation |
| 009fwd | Backward | Anticlockwise | 83° | 74.77° |
| 015aft | Forward | Clockwise | 83° | 74.77° |

[*]Looking from behind the satellite.

Initially, the panoramic camera model in the Socet Set™ software package was used to establish the geometric relationship between the stereo pairs. However, the best results using the rigorous approach of the available sensor modelling gave a uniform error of around 160 pixels to all points of one image and about 20 pixels to all points in the other image. In particular, the total RMSe was about 20m in each direction but the specific residuals were more than 1,000 m. The reasons for this error are unknown. It is possible the error comes from the panoramic camera parameters many of which are not known precisely because of the declassification process. The values of some of the parameters such as orientation angles can play an important role in the analysis. Unfortunately, the algorithms of the panoramic model used by Socet Set are not known, thus it was not possible to understand or explain the source of our large errors. After personal communication with Pournelle and Hunt (2002) who tried all available models (even SocetSet), it seems that the available panoramic film models, like those for frame cameras, presume boundaries on altitude and incidence angles that cannot work for orbital satellite platforms. Thus, the models presume a trapezoidal reprojection, which is not the case with CORONA.
ERDAS OrthoBase Pro is a module included in the ERDAS Imagine software. Like Socet Set, it includes sensor modelling to establish the internal characteristics associated with a specific camera or sensor with its main purpose being the orthorectification of the imagery. However, ERDAS has no panoramic camera model and so the only option is to use the non-metric camera model. In the non-metric camera model, the minimum requirements are an approximate focal length and the scanning resolution used to digitise the film. The coordinate system is defined according to the GCPs. The most difficult task was to allocate common points between the IKONOS imagery and the CORONA imagery because of the 30 year time difference and

---

[1] One of the main sites of archaeological interest in the area is the *tell*. It looks like a small hill and stands out nicely on the flat landscape.

physical changes to the landscape. It was also difficult to find common points between the maps and the IKONOS imagery. The first step was registration of CORONA to IKONOS and maps to IKONOS with the use of the Geometric Correction tool of ERDAS Imagine; thus identifying the GCPs. The height information was derived from the maps, using simultaneous display of the three data sources (maps, CORONA, IKONOS).

Afterwards, it was straightforward to put the same points in the CORONA imagery and create a first approximation of the geometric relationship between the image and the ground. The next step was the automatic tie point creation, which produced excellent results. A summary of the results is presented in Table 3.

**Table 3 - Summary of the stereopairs evaluation**

|  | **007-013** | **008-014** | **009-015** |
|---|---|---|---|
| Nº of tie points/GCPs | 14/11 | 21/11 | 0/13 |
| Minimum, maximum error | -7.243 m, 5.715 m | -10.846 m, 10.506 m | -7.622 m, 3.816 m |
| Mean error, mean absolute error | -0.864 m, 2.766 m | -0.732 m, 3.624 m | -1.726 m, 2.905 m |
| RMS error, LE90, NIMA LE90 | 3.377, 5.476, ± 3.189 | 4.461, 6.188, ± 4.280 | 3.830, 7.014, ± 4.109 |
| General mass point quality | 71.81% Vs 28.19% | 70.42% Vs 29.58% | 67.03% Vs 32.97% |

## 5    AUTOMATIC DEM EXTRACTION

ERDAS OrthoBase Pro automatically creates a DEM in three steps. First, it applies a digital image matching for DEM mass point collection. With the use of Förstner interest operator (Förstner and Gülch, 1987), it identifies a series of feature points such as road intersections or centres of circular features on each image (left and right) of the pair. The cross-correlation coefficients are calculated for each matching feature point, and the points with the higher correlation (0.8-1.0) are chosen as a matching pair. In other words, it utilises feature-based matching technique, but it is also looking at the topological and geometrical relations among the features. The parameters of the digital image matching can be customised according to each user's needs. Among the parameters, the search window size, the correlation window size and the correlation coefficient limit have the most influence.

The second step is the ground point coordinate determination. From the first step, a set of points is chosen in the left and right images. With the use of the space forward intersection technique, the ground coordinates of the points are computed to produce the mass points, which are then used as a basis for the third step, the DEM construction.

Before beginning DEM extraction, some common parameters were applied to all stereopairs. A trim frame of 2.5 % is applied to all overlaps. The trimming occurs after the mass points are extracted and before the DEM generation. Thus, the DEM is clipped to remove less accurate edges. The correlation area is reduced by a 5 % frame, thus preventing the extraction of erroneous mass points that may be present at the edges of the images. The reduction occurs before the mass points extraction.

The DEM image file pixel size was chosen to be 17 m to enable a minimum interest operator size[2]. The contour line spacing was chosen to be 10 m. Because of problems caused in the DEM extraction, all clouds and their shadows were excluded from the extraction, and they appear as black "islands" in the DEM. The extraction strategy was chosen to be *flat areas*[3] strategy with *adaptive change* applied.

## 6    ASSESSMENT AND DISCUSSION

During September 2002 Bridgland *et al.*(2003) used DGPS points to measure river terrace features. They established their points with the use of a base GPS of known coordinates and a "rover" GPS. Because these points were not taken from 'sensitive' areas (crossroads, bridges, etc.), the Syrian authorities allowed their use. For the same reason, it is impossible to identify these points precisely on the imagery. However, it was possible to detect these points from their Easting and Northing coordinates, and then compare their height with the height information taken from the CORONA data stereopair. The correlation was $r = 0.9954$ and the spatial distribution showed no systematic error or offset. Polidori (2002) points out that it is difficult to assess the accuracy and quality of a DEM in a quantitative way but suggests that the following criteria / questions are important (i) are the number of reference points good enough for the validation of the DEM extraction?; (ii) what errors may be associated with the reference points?; (iii) what level of accuracy is required for the application?; and are data of sufficient quality available to validate the results?

In this study the number of reference points obtained was the best possible under the circumstances. Raw IKONOS Geo product imagery was used as a horizontal reference; the contour lines of the maps were used as a height reference. Because of the difference in time and information content between the historical CORONA and modern IKONOS

---

[2] The methodology of the software for the DEM extraction requires a DEM cell size equal or higher to the maximal correlation window size, whose side has size of 7 pixels. Thus, the DEM cell size could not be less than 7 pixels size.
[3] In flat areas strategy, the search size is 7 x 3 pixels, which is adequate because of the absence of errors caused by high relief.

imagery, it was very difficult to define common identifiable points. This is a practical limitation of the method and its impact will vary from place to place depending on the degree of land cover change.

To address Polidori's question, the maps were registered to the IKONOS Geo product and so there is a horizontal error included in the height data. The difference in the scan mode (see table 2) may incorporate extra errors. It should be also noted that in the case of the 008-014 stereopair, some of the reference points were sampled from the registered-to-IKONOS CORONA imagery, because of the lack of adequate control for the triangulation process. Therefore, any geometric registration errors will be transferred to the DEM extraction. Perhaps this explains the magnitude of error in this stereopair in comparison with the other two (see table 3), even though this pair used more reference points than the other two stereopairs.

The third question explores the issue of the precision of the DEM and its appropriateness for the given application. In this case archaeologists are aware of upstanding monuments such as tells and natural landscape features such as river terraces of known height. It is important to know if such features could be identified on automatically extracted DEMs. Figure 3 demonstrates the limitations in scale of the automatically extracted DEM. Archaeological features such as tells are not easily identifiable, while landscape features such as river channels can be distinguished.



**Figure 3 - Identification of archaeological features (left) and detection of river channels (right)**

The last question explores the availability of independent height information that can be used to validate the results. Most published papers adopt a statistical approach for describing the quality of the DEM. This usually takes the form of statistics such as RMSE, mean error and absolute error which only relate to a few measured control points. Some authors are more rigorous and use independent control points. In this study we did not have the luxury of large numbers on ground control points and so reporting accuracy in this way (see table 3) may be very misleading because of the small number of reference points and the hidden errors. Fortunately, the DGPS points can be used as independent checkpoints, and these provide a helpful validation of the results even if these data are limited in this study. An alternative approach is to compare the DEM with height information that has been derived from an alternative method such as photo interpreted contour lines and Shuttle Radar Topography Mission (SRTM) data.

For the comparison of the SRTM and CORONA DEMs, the ERDAS Imagine utility 'change detection' was used (or 'image differencing'). This utility reads the pixel values from two images which are assigned as 'before image' and 'after image', and produces a third image from their subtraction in the formula: *Before image – After image = Final image*. The final image gets the smaller pixel size (in our case, the CORONA DEM, 17m) and its boundaries are defined by the use of AOI (Area Of Interest) layer. The SRTM DEM was assigned the 'after image' character, and the CORONA DEM the 'before image'. In table 4, the minus differences mean higher SRTM pixel values, while the plus differences show higher CORONA pixel values.

The results show large differences at the edges (maximum-minimum) of the points' distribution. However, this applies to a very small number of points and this can be seen from the statistic of the percentage of pixels within one standard deviation of the mean DEM altitude. The mode of the distribution shows less than a metre difference, and the mean altitudinal differences for the three DEMs are 3.30, 2.24 and 1.30 metres respectively. This shows a very good fit between the SRTM-3 and the CORONA DEMs. Some caveats were noticed in SRTM-3 DEM of the Homs area. A few areas were blank of data, and where the river has steep banks (north part of 007013 stereopair) the height values were anomalous.

**Table 4 - Statistics of the differences of CORONA DEM – SRTM-3**

| Statistics | 007013-SRTM | 008014-SRTM | 009015-SRTM |
|---|---|---|---|
| Maximum (m) | 128.57 | 89.43 | 92.39 |
| Minimum (m) | -125.97 | -93.27 | -50.74 |
| Mean (m) | 3.30 | 2.24 | 1.30 |
| Median (m) | 1.98 | 1.32 | -0.59 |
| Mode (most frequently occurring) | -0.70 | 0.34 | -0.47 |
| Standard Deviation | 8.98 | 7.97 | 5.03 |
| Pixels in one standard deviation | 81.36% | 71.94% | 77.37% |
| Total overlap number of pixels | 1125898 | 1064586 | 1269917 |

An interesting approach is to map the spatial behaviour of the errors. Horizontally, this can be illustrated with a display of the GCPs fit error and its direction. Vertically, this can be illustrated with comparisons through overlap of the resulting DEM with other DEMs or independent check points. The spatial behaviour of the errors may not give any quantitative evaluation, but proves to be very useful qualitative guide to accuracy.

## 7    CONCLUSIONS

The research has demonstrated that it is important to be aware of CORONA image characteristics which might impact on photogrammetry. No two CORONA missions were the same and in many missions with stereoscopic capability, the two camera systems (aft and forward) were not the same.

If scanned with care, the CORONA image quality provides high levels of detail on ground features. The scanning should be done using a photogrammetric scanner for best geometric and radiometric results. The geometric precision of the scanning should be done in balance with the radiometric precision if the user wishes to get the most from the imagery. Also, the scanner should be sufficiently calibrated and the scanning parameters should be kept the same between image pairs. However, the detail and process of digitising of CORONA imagery depends on the application. When the preprocessing is done with care and there is understanding of the data, then three-dimensional information can be extracted from CORONA imagery using only a small number of GCPs. If good quality map data are not available, the horizontal location of GCPs can be obtained from IKONOS Geo product satellite imagery. In this study, height information was derived from maps, although points fixed from a Differential GPS can also be used and may even improve the accuracy of the model.

The methods described here were not expected to yield excellent results because of the limited amount of ground control that was available. However, the CORONA DEM data compares well with other sources of height data which suggest that the data are useful. Results show that the methodology is robust and so it would be interesting to test the approach in other areas where ground control is difficult to obtain. Satellite ephemeris and attitude data, and specialist panoramic image processing software, all of which are difficult to obtain, are not in fact necessary.

## 8    ACKNOWLEDGEMENTS

## 9    REFERENCES

Altmaier, A., and Kany, C. (2002), Digital surface model generation from CORONA satellite images, *ISPRS Journal of photogrammetry and remote sensing*, vol. 56, No. 4, pp. 221-235.

Beck, A.R., Philip, G., Donoghue, D.N.M., and Galiatsatos, N., (in press), Geo-locating declassified CORONA satellite photography for archaeological surveys and cultural resource management applications: an interim paper, *Workshop on aerial archaeology and remote sensing*, Siena, Italy.

Bindschadler, R., and Vornberger, P., (1998), Changes in the west Antarctic ice sheet since 1963 from declassified satellite photography, *Science*, vol.279, 30th January, pp.689-692.

Bridgland, D.R., Philip, G., Westaway, R., and White, M., (2003), A long Quaternary terrace sequence in the Orontes river valley, Syria: a record of uplift and of human occupation, *Current Science*, vol.84, No.8, pp.1080-1089.

Case, J.B., (1967), The analytical reduction of panoramic and strip photography, *Photogrammetria*, p.127-141.

Day D.A., Longson J.M., and Latell B. (eds.) (1998), Eye in the sky – The story of CORONA spy satellites, Smithsonian Institution Press, Washington and London.

Deveraux, Jr. A.B., (1973), Investigations into the feasibility of employing a hypothetical panoramic-frame camera system in aerial triangulation, PhD submitted in the Geodesy department of The Ohio State University.

Förstner, W., and Gülch, E., (1987), A fast operator for detection and precise location of distinct points, corners and centers of circular features, *Intercommision conference on fast processing of photogrammetric data*, Interlaken, Switzerland, pp.281-305.

Fraser, C.S., Hanley, H.B., and Yamakawa, T., (2002a), Three-dimensional geopositioning accuracy of IKONOS imagery*, Photogrammetric record*, vol. 17, No. 99, pp. 465-479.

Galiatsatos, N., (2004), Assessment of the CORONA series of satellite imagery for landscape archaeology: a case study from Orontes valley, Syria. Dissertation for the degree of Doctor of Philosophy, University of Durham, United Kingdom.

Goossens, R., Schmidt, M., Altmaier, A., Benoit, F., and Menz, G., (2001), Extraction of Digital Elevation Models and ortho-images from CORONA KH4B data, *Proceedings of ISPRS Workshop: High resolution mapping from space*, Hannover, Germany.

Goossens, R., (2004), personal communication.

Madden, F.J., (1996), The CORONA camera system: Itek's contribution to world stability, self-published.

Leachtenauer, J.C., Daniel K., and Vogl, P.T. (1997), *Digitising Corona Imagery: Quality vs. Cost*. In McDonald, Robert A., (ed.) (1997), *Corona Between the Sun and the Earth The First NRO Reconnaissance Eye in Space*, American Society for Photogrammetry and Remote Sensing, Bethesda, MD

McDonald, R.A., (ed.), (1997) CORONA Between the Sun and the Earth The First NRO Reconnaissance Eye in Space, American Society for Photogrammetry and Remote Sensing, Bethesda, MD.

National Reconnaissance Office (NRO), (1970a), CORONA technical information volume 1, National Photographic Interpretation Centre, December 1970.

National Reconnaissance Office (NRO), (1970b), CORONA technical information volume 2, National Photographic Interpretation Centre, December 1970.

Ondrejka, R., (2000), personal communication.

Palmer, R., (2002), A poor man's use of CORONA images for archaeological survey in Armenia, *Proceedings of the conference: Space applications for heritage conservation*, Strasbourg, France.

Peebles, C., (1997) The CORONA project: America's first spy satellites, Naval Institute Press, Annapolis, Maryland.

Philip, G., Jabour, F., Beck, A., Bshesh, M., Grove, J., Kirk A., and Millard, A., (2002), Settlement and landscape development in the Homs region, Syria: research questions, preliminary results 1999-2000 and future potential. *Levant*, 34, pp.1-23.

Polidori, L., (2002), DSM quality: Internal and external validation, in: Kasser, M. and Egels, Y., (eds.), *Digital Photogrammetry*, Taylor and Francis: London and New York.

Pournelle, J., and Hunt, L., (2002), personal communication.

Ruffner, K. (ed.), (1995), CORONA: America's First Satellite Program, Center for the Study of Intelligence, Government Printing Office, Washington D.C.

Schenk, T, Csathó, B., and Shin, S.W., (2003), Rigorous panoramic camera model for DISP imagery, *Proceedings of the ISPRS Workshop "High resolution mapping from space"*, Hannover, Germany.

Schmidt, M., Goossens, R., and Menz, G. (2001a), Processing techniques for CORONA satellite images in order to generate high-resolution digital elevation models (DEM), In: Begni, G., (ed.), *Observing our environment from space: New solutions for a new millennium*, Lisse, The Netherlands, pp. 191-196.

Schmidt, M., Goossens, R., Menz, G., Altmaier, A., and Devriendt, D., (2001b), The use of CORONA satellite images for generating a high-resolution digital elevation model, *Proceedings of the 2001 IGRASS Symposium*, Sydney.

Shin, S.W., (2003), Rigorous model of panoramic cameras. Dissertation presented in partial fulfilment of the requirements for the degree Doctor of Philosophy. Department of civil and environmental engineering and geodetic science, Ohio State University, 104 p.

Slama, C.C., Theurer, C., and Henriksen, S.W., (eds.) (1980), Manual of Photogrammetry, American Society of Photogrammetry.

Sohn, H.G., Kim, G., Yom, J., (2004), Mathematical modelling of historical reconnaissance CORONA KH-4B imagery, *The photogrammetric record*, vol.19, issue 105, pp. 51-66.

Tappan, G.G., Hadj, A., Wood, E.C., and Lietzow, R.W., (2000), Use of Argon, Corona and Landsat imagery to assess 30 years of land resource changes in west-central Senegal, *Photogrammetric engineering and remote sensing*, vol.66, No.6, pp.727-735.

Thom, C., (2002), Relations between radiometric and geometric precision in digital imagery, in: Kasser, M. and Egels, Y., (eds.), *Digital Photogrammetry*, Taylor and Francis: London and New York.